Chapter 3

Evaluation of Physical Tissue Compensation Filters

The prime purpose of this project was to develop and evaluate a method to digitally alter the dynamic range of digital radiographic images. This digital manipulation of the dynamic range can achieve alteration of the displayed contrast and brightness of the digital radiographic image, based on the underlying anatomy within the image. So-called anatomically shaped radiographic contrast-enhancement masks (RCMs) are based on the physical characteristics of physical tissue compensation filters (TCFs). Evaluation of the TCFs was an integral step to gain knowledge of these characteristics prior to development of the anatomically shaped RCMs.

TCFs are x-ray attenuating material of non-uniform shape, which are placed in the x-ray beam prior to the beam reaching the image receptor. The purpose of the TCF is to compensate for anatomical differences in x-ray attenuation that cause large variations in optical density (OD) on the radiographic film. TCFs reduce the range of OD on the resulting radiographic film and enable radiographic contrast to be optimised for the anatomical region of interest.

Many authors have commented on the clinical use of TCF in radiographic examinations (Bushong, 2001; Butler *et al*, 1986; Crow *et al*, 1983; Curry *et al*, 1990; Feczko *et al*, 1983; Gray, Hoffman & Peterson, 1983; Marugg *et al*, 1990; Petersen & Rohr, 1987; Thompson *et al*, 1994; Vezina, 1985). TCFs have been found useful in a variety of film/screen (F/S) general radiographic examinations. Anatomical regions where TCFs have been used include the shoulders, spine, decubitus abdomen projections, chest, hands, feet and the lower legs.

Many different shapes of TCF have been designed and reported for use with specific anatomical regions. Vezina (1985, 1995) discussed a boomerang shape for use with shoulder radiographic examinations. A variety of wedge shapes have been discussed by Bushong (2001), Butler *et al* (1986), Crow *et al*, (1983), Gray, Stears & Frank (1983), Thompson *et al* (1994) and Vezina (1995). Trough shaped filters were investigated by Thompson *et al* (1994) and Bushong (2001). Ingot shaped filters

were discussed by Vezina (1995). Marugg *et al* (1990) suggested that multiple filters could be used during the same radiographic exposure to form complex shapes. As part of a comparison of chest x-ray imaging techniques, Müller *et al* (1996c) examined the use of specially shaped filters for the lung regions. Goodsitt *et al* (1998) developed various TCF shapes for use in mammography.

3.1 Tissue Compensation Filter Material

Any material that attenuates the x-ray beam can be used for construction of TCFs. Vezina (1995) lists material including rice, flour, water bags, some types of plastic and many metals that can be used to compensate for so-called over-penetration of the anatomical region. Coupled with compensation for over-penetration, x-ray exposure factors can be adjusted to compensate for so-called under-penetration of the anatomical region. According to Bushong (2001), compensating filters are commonly constructed of aluminium, but plastic materials are sometimes used. Other authors have reported the use of aluminium (Al) TCF (Butler *et al*, 1986; Crow *et al*, 1983; Feczko *et al*, 1983; Katsuda, Okazaki & Kuroda, 1996; Müller *et al*, 1996c). Vezina (1985, 1995) discussed TCFs constructed of silicone rubber. Silicone rubber has attenuation characteristics twice that of human muscle (Vezina, 1995). Lead acrylic filters have been described by Gray, Hoffman & Petersen (1983), Butler *et al* (1986), Petersen & Rohr (1987), Gray, Stears & Frank (1983) and Katsuda *et al* (1996).

Three common materials used in the construction of TCFs reported in the literature are aluminium, lead acrylic and silicon rubber. Due to the different attenuation characteristics of each of these materials, different thicknesses of the TCF material are required to produce a similar effect for the same radiographic examination.

In this study, TCFs typical of those reported in the literature were examined and thicknesses were measured. TCFs constructed from three different materials, silicone rubber, lead acrylic and aluminium composite, were purchased. The specific filters (model/brand name; material; shape and manufacturer) are listed in Table 3.1.

Table 3.1 Details of tissue compensation filters

Model / Brand Name	Material	Shape	Manufacturer
F700	aluminium composite	shoulder shaped	Grey Tech Services, Australia
F100	aluminium composite	wedge shaped	Grey Tech Services, Australia
F600	aluminium composite	double wedge shaped	Grey Tech Services, Australia
Gentle Slope	silicone rubber	wedge shaped	Octostop, Canada
Little Prism	silicone rubber	wedge shaped	Octostop, Canada
Clear-Pb – 57-415	lead acrylic	edge shaped	Nuclear Associates, USA

Aluminium composite TCFs are shown in Figure 3.1a & b. Model F700, in Figure 3.1a (A) is typically used for radiographic examinations of the shoulder. This TCF has dimensions of 80 mm x 40 mm in plan view and a maximum thickness of 11 mm. Model F100, shown in Figure 3.1a & b (B), has a variety of uses in radiographic examinations. This TCF has dimensions of 135 mm x 78 mm in plan view and a maximum thickness of 10 mm. Model F600, shown in Figure 3.1a & b (C) has wedge shapes to each side, and is typically used in radiographic horizontal ray examinations of the abdomen and hips. Its dimensions are 79 mm x 53 mm in plan view and a maximum thickness of 15 mm (centre). The composition of the Al composite material was not available from the manufacturer.

Silicone rubber TCFs are physically larger than Al composite TCFs. The two silicone rubber TCFs can be seen in Figure 3.2a & b. Model “Gentle Slope”, shown in Figure 3.2a & b (A), has dimensions of 297 mm x 165 mm in plan view and a maximum thickness of 20 mm (top as visualised). The slope of the wedge is at an angle of 8º (from the bottom to top as visualised). This TCF would be typically used

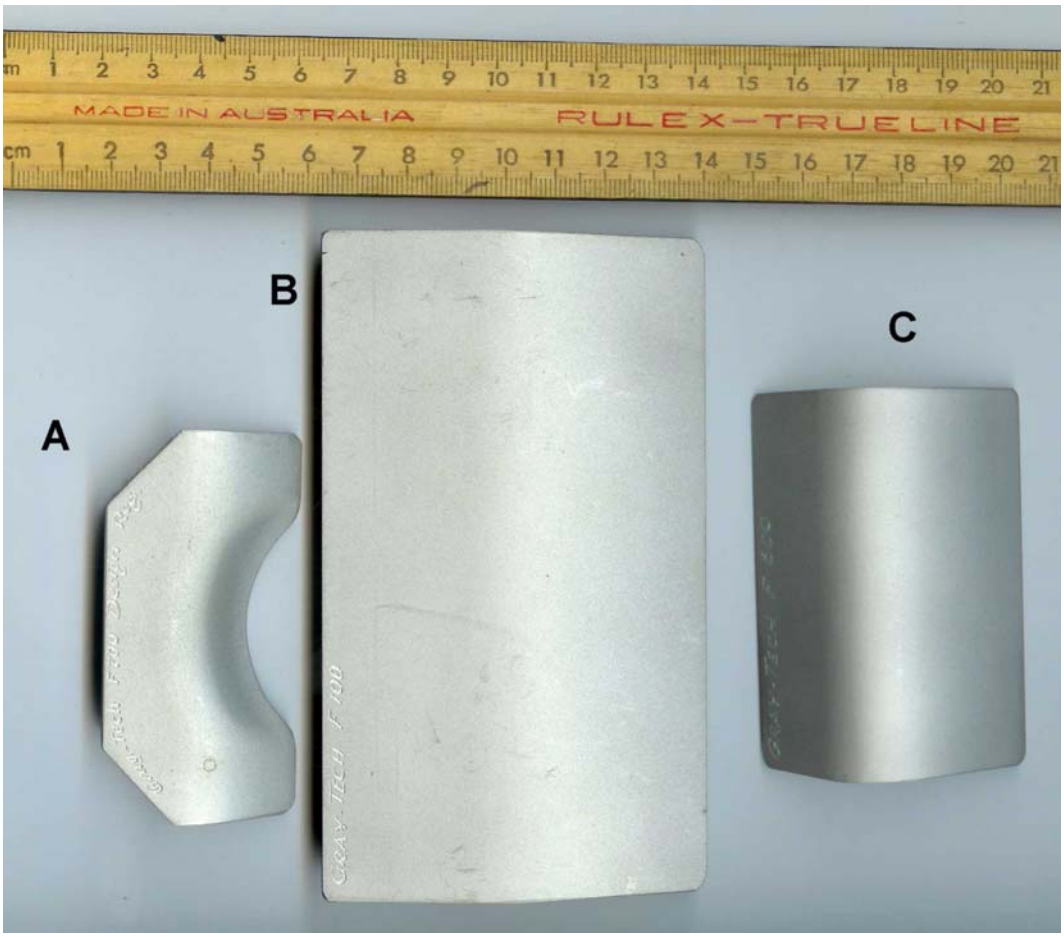

a.

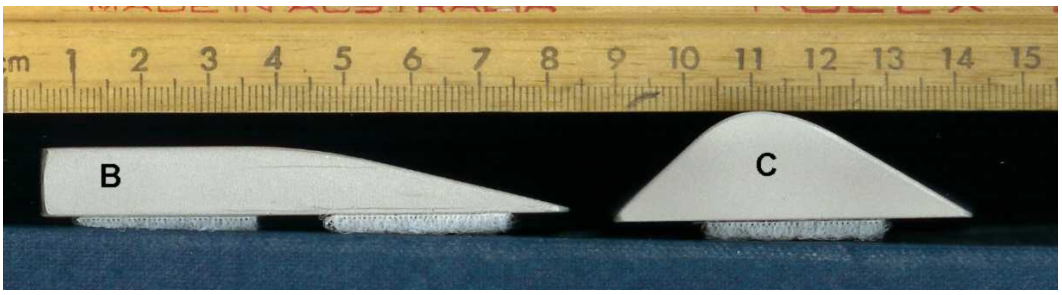

b.

Figure 3.1 Aluminium composite TCFs; Grey Tech Services (Australia):
a. Plan view; b. Side view (Velcro tape seen underneath)
Models are: A. F700; B. F100; C. F600

for radiographic examinations of the hands and feet. Model "Little Prism", shown in Figure 3.2a & b (B), is also a double wedge sloping top to bottom as visualised. It has dimensions of 206 mm x 78 mm in plan view and a maximum thickness of 36 mm (top as visualised). The slopes of the wedge are at an angle of 37º (the bottom as visualised in a. and right as visualised in b.) and 52º (the top as visualised in a. and

left as visualised in b.). This TCF would be used in horizontal ray radiographic examinations of the abdomen.

Lead acrylic attenuates x-ray photons to a greater extent than aluminium composite or silicon rubber. Therefore the thickness of the lead acrylic TCF required to achieve the same x-ray photon attenuation is much less than that of aluminium composite or silicon rubber materials. The lead acrylic TCF, Model "Clear-Pb 57-415", as shown in Figure 3.3a & b, has dimensions of 165 mm x 105 mm in plan view and a maximum thickness of 3 mm of lead acrylic (top as visualised in 3.3a.). The filter has two sections; a uniform 3 mm thick section (indicated by arrows in Figure 3.3a. and indicated by arrows on the left side in Figure 3.3b.) and a wedge section (bottom of the filter in Figure 3.3a. and indicated by arrows on the right side in Figure 3.3b.). A side view of the lead acrylic TCF is shown in Figure 3.3b. The arrows show the lead acrylic TCF's uniform thick and wedge sections embedded in an acrylic material for support. Magnet strips are visualised at the sides of the TCF for attachment to the x-ray collimator. The overall thickness of plain acrylic and lead acrylic is 10 mm. This TCF would be used for radiographic examinations of the spine and legs.

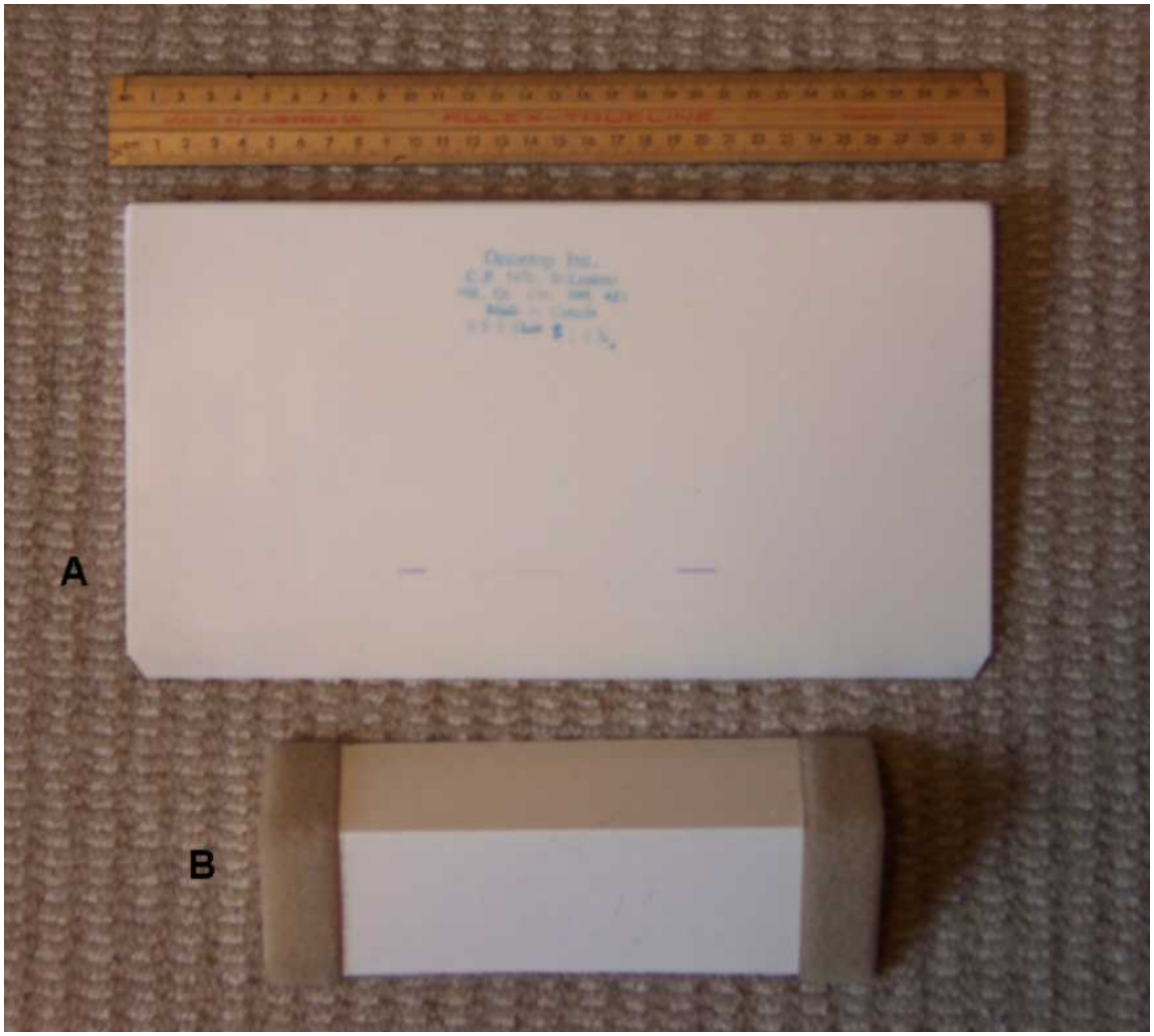

a.

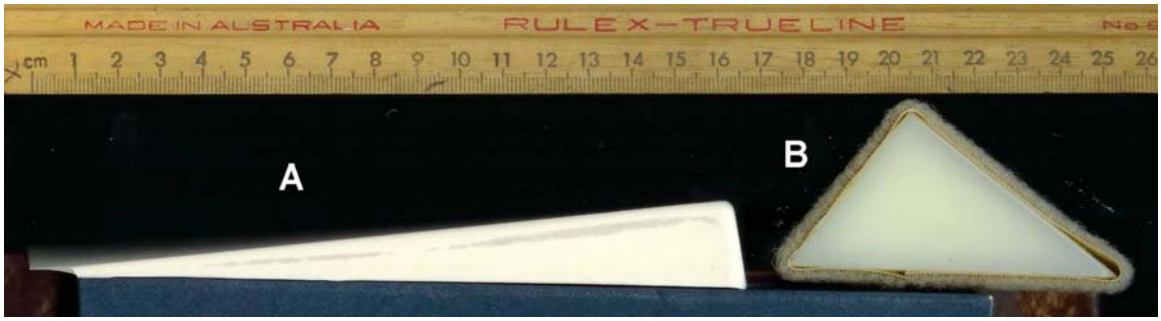

b.

Figure 3.2 Silicone rubber TCFs; Octostop (Canada): a. Plan view; b. Side view

Models are:- A. Gentle slope

B. Little Prism with velcro at each end

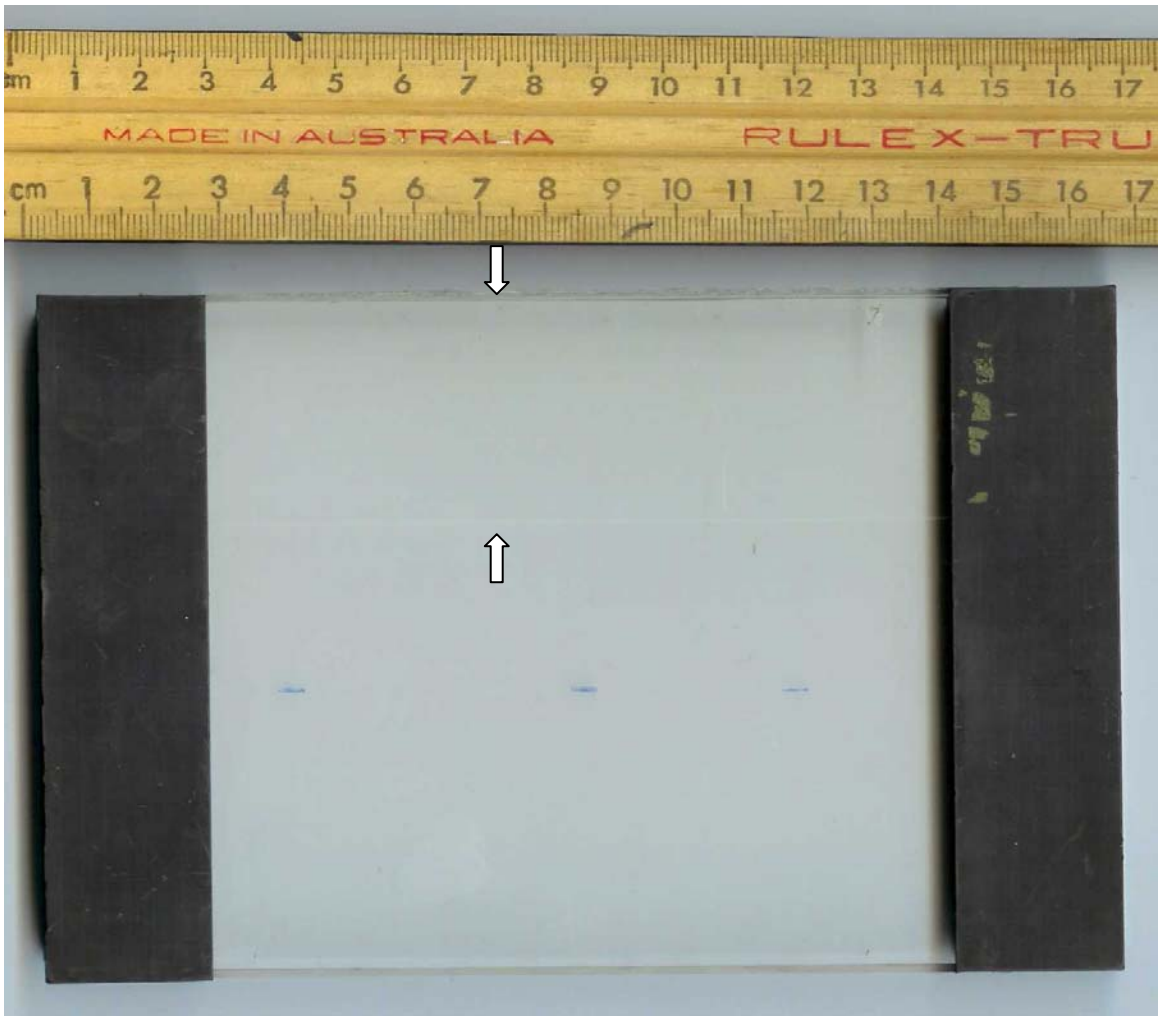

a.

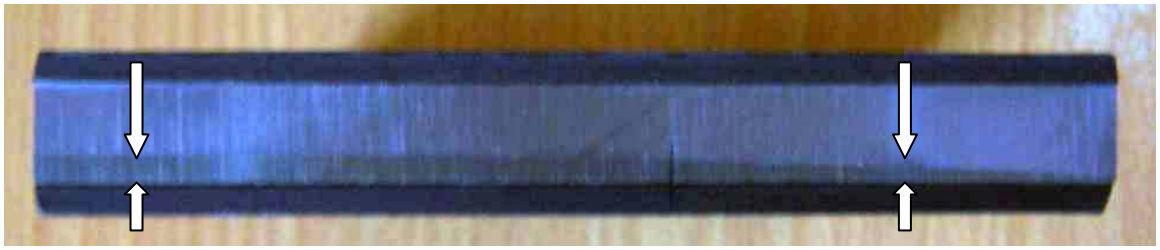

b.

Figure 3.3 Lead acrylic TCF, Nuclear Associates (USA):

a. Plan view with ruler – Arrows show section of uniform thickness. Black magnetic strips are seen on both sides.

b. Side view – Arrows show lead acrylic section within a thicker acrylic layer and two black magnetic strips (top and bottom)

TCFs are generally placed in the x-ray beam following the x-ray beam's exit from the x-ray tube and collimator and prior to the beam's entrance into the patient (Bushong, 2001; Thompson *et al*, 1994). Vezina (1985, 1995) describes an alternative placement of the silicone rubber TCF, which may be placed in the x-ray beam following its exit from the patient's anatomy and prior to the x-ray beam reaching the image receptor. Silicone rubber TCFs are larger than lead acrylic and aluminium composite TCFs, due to their attenuation characteristics. The appropriate placement of lead acrylic and aluminium composite TCFs, given their small physical size, is in close proximity to the x-ray beam prior to its divergence. Use of the silicone rubber TCF is more appropriate, where the x-ray field is larger, at a greater distance from the x-ray tube compared to lead acrylic and aluminium composite TCFs. Placement of a silicone rubber boomerang shaped TCF between the patient and the film can be seen in Figure 3.4 (Vezina, 1995).

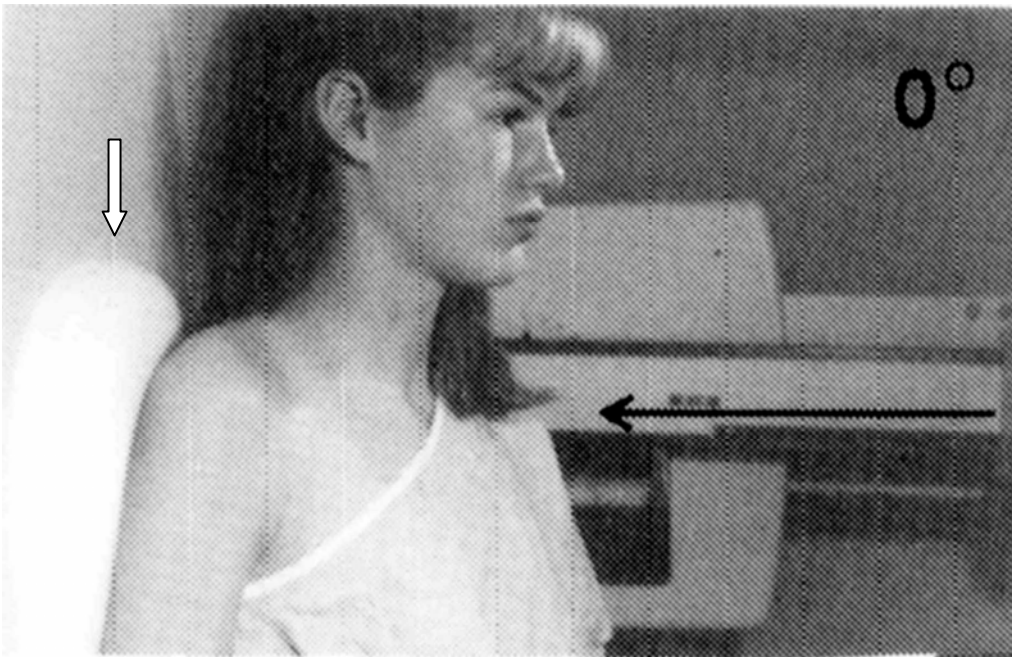

Figure 3.4 Boomerang shaped TCF (white arrow) positioned between the patient and film. Black arrow depicts direction of the x-ray beam (Vezina, 1995, p. 823)

3.2 Absorbed Dose and Tissue Compensation Filters

Reduction of absorbed dose through the use of added filtration has been the topic of much research (Chakera *et* al, 1982; Cranage, Howard & Welsh, 1992; Gagne, Quinn & Jennings, 1994; Koedoorer & Venema, 1986; Konh, Gooch, & Keller, 1988; MacDonald-Jankowski & Keller, 1992; Shrimpton, Jones & Wall, 1988; Sandborg, Carlsson & Carlsson, 1994; Villagran, Hobbs & Taylor, 1978; Williamson & van Doorn, 1994). Reduction of absorbed dose is also considered when using TCFs (Butler *et al*, 1986; Feczko *et al*, 1983; Gray, Hoffman & Peterson, 1983; Gray, Stears & Frank, 1983; Katsuda *et al*, 1996).

Gray, Stears & Frank (1983) and Gray, Hoffman & Peterson (1983) reviewed absorbed dose when lead acrylic TCFs were used in examinations of the spine. Comparisons of absorbed dose were made with and without TCF present in the x-ray beam. The conclusions reached were that appropriately applied lead acrylic TCFs could reduce absorbed dose to the breast by a factor of 25 – 55 times and to the thyroid by a factor of up to 103 times. Butler *et al* (1986) also concluded that the use of both lead acrylic and aluminium composite TCFs reduced dose to the breast during radiographic examinations of the scoliotic spine. No comparison of the dose reduction ability between lead acrylic and aluminium composite TCF was reported.

Katsuda *et al* (1996) examined dose reduction in other anatomical areas. They found a 29% reduction of absorbed dose to the skull and a 47% reduction of absorbed dose to the upper abdomen when aluminium composite TCFs were used. When a lead acrylic TCF was used during the radiographic examination of the lower extremities, Katsuda *et al* found that an 80% absorbed dose reduction was achieved.

Aluminium and Plexiglas were used as the TCF material in radiographic examinations of the decubitus abdomen (Feczko *et al*, 1983). Three TCFs were used: an aluminium composite TCF with a maximum thickness of 12.5 mm and Plexiglas TCFs with maximum thicknesses of 65 mm and 95 mm. (Cross-sections of these TCFs were shown in Figure 2.6.) The aluminium composite and 65 mm Plexiglas

TCF both achieved dose reductions of 14% compared to doses without. The 95 mm Plexiglas TCF dose reduction was 19%.

TCF material can only achieve a dose reduction if the TCF is placed in the x-ray beam prior to the x-ray beam entering the patient. No dose reduction advantages will be experienced by the patient when the TCF is placed between the patient and the image receptor.

3.3 Comparison of TCF Materials

Butler *et al* (1986), Katsuda *et al* (1996) and Feczko *et al* (1983) reported on the use of different TCF materials. Katsuda *et al* (1996) did not make direct comparisons between TCF materials in the same anatomical region. In the examination of the scoliotic spine, Butler *et al* (1986) used TCFs consisting of aluminium composite and lead acrylic. Results of image quality improvements and dose reduction were reported.

Feczko *et al* (1983) compared TCF materials of aluminium and Plexiglas in the horizontal ray radiographic examination of the decubitus abdomen. When the 95 mm Plexiglas TCF was used, radiographic examination quality was considered “much better” in three of ten examinations and “better” in seven of ten examinations assessed by these authors. In examinations where the aluminium TCF was used, quality was considered “much better” in three, “better” in seven and “the same” in one examination. The 65 mm Plexiglas produced quality changes of “much better” in five, “better” in four and “the same” in one examination.

Not all characteristics of TCF materials have been investigated in the literature. Knowledge of characteristics of half value thickness (HVT) and linear attenuation coefficients of different TCF material would assist radiographers in the appropriate selection of a TCF.

3.4 X-ray Equipment Used for TCF Measurements

In this study, measurements of exponential attenuation rates and HVT of different TCF materials were made. Parameters that quantify the attenuation rates of materials are their linear attenuation and mass attenuation coefficients. These quantities are dependent on photon energy and are quoted at a specific photon energy (Bushberg *et al,* 2002; Bushong, 2001; Curry *et al*, 1990; Thompson *et al*, 1994). A method of measuring the photon energies within the x-ray beam was therefore required for reporting of the attenuation coefficients.

Comparisons of the spectra of x-ray beams with various thicknesses of TCF material and without any TCF in the x-ray beam were made using clinical radiographic x-ray equipment. The clinical x-ray units used were Unit 1: Toshiba KXO-30R (Toshiba, Australia); Unit 2: Toshiba KXO-850 (Toshiba, Australia) and Unit 3: Toshiba KXO-15R (Toshiba, Australia).

An x-ray generator converts low voltage power supply (in Australia, 415V three phase RMS) to the very high peak kilovoltages required for x-ray production. Various x-ray generator types are available for clinical use. The *ripple factor*, expressed as a percentage, provides an indication of the voltage variations from the peak voltage during a given time period or alternating wave cycle. A high ripple percentage implies a greater variation of voltages within the wave cycle that is used for x-ray production. Ripple percentage also provides an indication of the quality of the output of the x-ray generator. A high ripple percentage implies a greater amount of low energy photons in the x-ray beam and a greater absorbed dose to the patient. X-ray beam attenuation is greater in higher ripple factor x-ray generators due to the greater number of low energy photons in the beam. Radiographers must increase radiographic exposure factors to produce the same optical densities on the film when using an x-ray unit with 100% ripple compared to an x-ray unit with a small ripple factor (Bushong, 2001; Curry *et al*, 1990; Thompson *et al*, 1994).

Figure 3.5 (Thompson *et al*, 1994) provides a graphical representation of x-ray generator ripple. In Figure 3.5, the top plot is a diagrammatic representation of a

single phase voltage supply. The lower three plots show diagrammatic representations of x-ray generator ripples of 100%, 13.5% and 3.5% respectively (note that in Australia the mains frequency is 50Hz rather than 60Hz as shown in Figure 3.5).

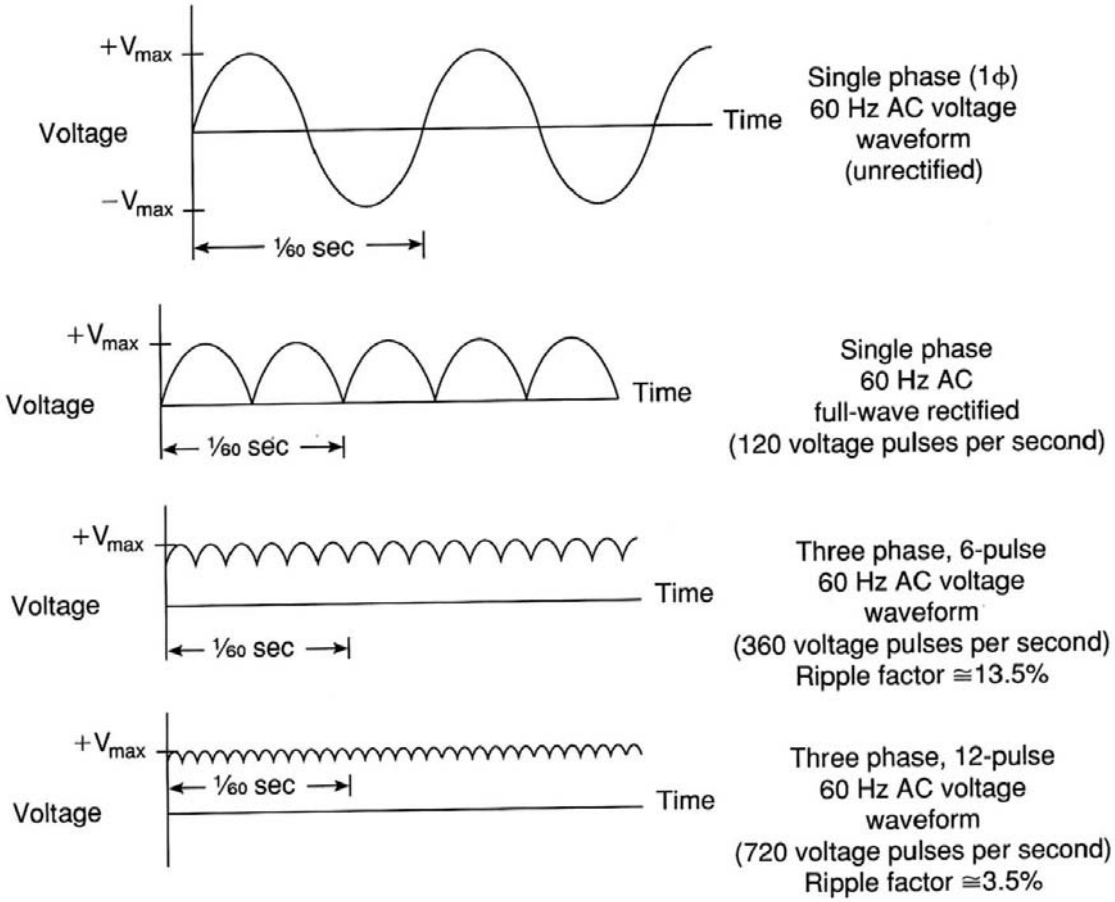

Figure 3.5 Voltage ripple in x-ray production (Thompson *et al*, 1994, p.169)

Other determinants of radiation quality for an x-ray unit are the amount of added filtration and measurements of the HVT. Absorbed dose to the patient is reduced when there is a greater amount of added filtration and hence a larger measurement of HVT (Bushong, 2001; Curry *et al*, 1990; Thompson *et al*, 1994).

Specification of the three x-ray units used in the measurement of TCF spectra can be seen in Table 3.2. The three units were typical of clinical x-ray units.

Table 3.2 Specification of the three clinical x-ray units

	Generator Type	Generator Ripple (approx.)	Filtration 1. Inherent 2. Added	HVT @ 75kVp (mm Al)
Unit 1	single phase, medium frequency	1%	1. 0.7 mm Al 2. 1.1 mm Al	5.20
Unit 2	three phase, 12 pulse	3.5%	1. 0.7 mm Al 2. 1.1 mm Al	3.91
Unit 3	single phase, 2 pulse	100%	1. 0.7 mm Al 2. 2.2 mm Al	3.96

3.5 Measurement of X-ray Photon Energies

X-ray photon energies within the x-ray beam can be recorded using a high quality, low noise detector and multi-channel analyser (MCA). Clinical x-ray units produce very high intensity beams. A problem called *pulse pile-up* in the MCA can occur when recording x-ray beams from clinical x-ray units without some means of reducing the number of photons in the x-ray beam. Typical means of reducing the number of photons reaching the detector are to limit the size of the x-ray beam and to increase the distance between the source of the beam and the detector. When using clinical x-ray equipment this can be difficult to achieve (Matscheko, 1988; Matscheko & Ribberfors, 1987).

Matscheko (1988) provided an alternative means of reducing the number of photons reaching the detector, using a device called a *Compton spectrometer*. Within the Compton spectrometer, a Lucite rod is placed in the path of the x-ray beam. Compton spectrometers use the Lucite rod to reduce the number of x-ray photons reaching the detector by only allowing radiation scattered at 90º from the direction of the original x-ray to reach the detector. The problem of pulse pile-up can be overcome by the use of this method. The Compton spectrometer can be seen in Figure 3.6 and a diagrammatic representation in Figure 3.7 (Matscheko, 1988). As shown in Figure 3.7, the primary x-ray beam is directed through aperture (A) in the Compton spectrometer towards the Lucite rod (block arrow). Only scatter at 90º passes through the scatter chamber (F) to reach the detector (G).

Scatter radiation from Lucite is predominantly Compton scatter due to the low effective atomic number of Lucite (Matscheko & Ribberfors, 1987). After the Compton scatter has been recorded, the recorded photons must be deconvolved so as to represent the number and energy levels of the photons in the original x-ray beam. The Compton formula, used to relate the energies of the incident and scattered photons, is presented in Equation 3.1. Matscheko & Ribberfors (1989) used this formula to develop an algorithm to regenerate the original x-ray beam spectrum from the Compton spectrum.

$$E_{SC} = \frac{E_0}{1 + (E_0 / 511).(1 - \cos\theta)} \qquad \text{…….. 3.1}$$

where: E_{SC} is the energy of the scattered photon (keV);

E_0 is the energy of the incident photon (keV) *and*;

θ is the angle of the scattered photon.

(Bushberg *et al*, 2002)

Figure 3.6 Compton spectrometer

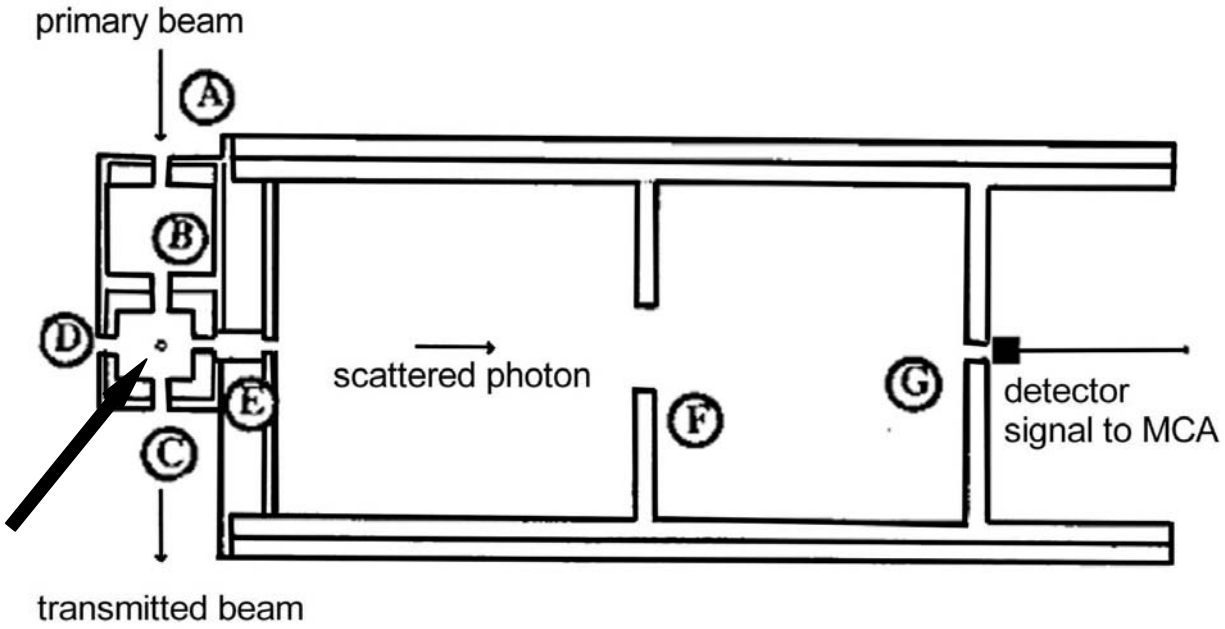

Block arrow indicates site of Lucite rod

A. Entrance - Primary beam
B. Scatter chamber - Primary beam
C. Transmitted beam
D. Line of sight
E. Pb shielding
F. Scatter chamber - Scattered photons
G. Detector aperture

Figure 3.7 Diagrammatic representation of the Compton spectrometer (Matscheko, 1988, p.39)

Lucite rods of different diameters are used in the Compton spectrometer. Matscheko & Carlsson (1989) reported on the effects of the use of various diameter (0.5 to 4.0 mm) Lucite scattering rods in the Compton spectrometer. The diameter of the rod affects the number of photons that are scattered. When the diameter of the rod is increased, the number of scattered photons increases. The disadvantage of increasing the size of the rod is that scattered photons reaching the detector may be at angles other than 90º. When the angle of the scattered photon is not at 90º, noise is introduced into the system resulting in reduction of the resolution of the reconstructed spectra (Matscheko, 1988; Matscheko & Carlsson, 1989;).

A Compton spectrometer, germanium (HPGe) detector (Canberra Nuclear, USA) and a MCA (APTEC, USA) were obtained from the Australian Radiation Protection and Nuclear Safety Agency (ARPANSA). The HPGe detector was required to be cooled by liquid nitrogen. The MCA was connected to a personal computer (PC) for the recording and storage of the x-ray Compton spectra. The PC was also used to

regenerate the original beam spectra from the Compton spectra using Matscheko's algorithm. The relationship between the x-ray tube, the Compton spectrometer, the HPGe and the liquid nitrogen Dewar can be seen in Figure 3.8.

X-ray spectra were recorded at peak kilovoltage (kVp) of 60, 70, 80, 90 and 100 kVp on the three clinical x-ray units. At each of these kVp settings and on each clinical x-ray unit, spectra were recorded using three thicknesses of each TCF material, lead acrylic, aluminium composite and silicone rubber, and without TCF material present in the x-ray beam.

Figure 3.8 Compton spectrometer and its relationship to the x-ray tube and HPGe. Lead sheeting is distal to the spectrometer to reduce backscatter

Thicknesses of TCF material for placement in the x-ray beam were selected on the basis of the maximum thickness of the TCF material available and two other thicknesses. The two other thicknesses were chosen where there was ease of measurement of the TCF material and for ease of placement of that thickness of TCF material in front of the spectrometer. The thicknesses of each TCF material are listed in Table 3.3.

Table 3.3 Tissue compensation filter material and thicknesses used in the spectral analysis

Filter Material	Thicknesses
Aluminium Composite	5 mm, 10 mm, 15 mm
Silicone Rubber	5 mm, 10 mm, 20 mm
Lead Acrylic	0.75 mm, 2 mm, 3 mm

The MCA had 2048 channels to record different photon energies. The energy range chosen was from 0.1 to 110 keV. Calibration of the MCA was required prior to the recording of the spectral data. An Americium source (^{241}Am) was chosen for the calibration as it has gamma radiation emissions within the diagnostic x-ray energy range at 26.37 keV and 59.57 keV (Weast, 1975).

3.6 X-ray Spectra of Tissue Compensation Filters

Test exposures without the presence of TCF material in the beam were made to evaluate the x-ray spectra. A radiographic exposure consists of three factors that are selectable by the radiographer: kVp, a combination of tube current and time (mAs), and distance from the source of the x-rays to the receptor (Fauber, 2000; Gunn, 2002). Test exposure factors selected were 100 kVp and 25, 50 and 100 mAs. Matscheko & Carlsson (1989) recommend a distance between the x-ray focus and the spectrometer of 20 cm rather than the typical 100 cm source to receptor distance used clinically. Test exposures were also made using various diameters of Lucite rods of 0.5 mm, 1 mm, 2 mm and 4 mm. Evaluation of these spectra found that the signal to noise ratio (SNR) was very low. Changes to the experimental factors were made to increase the SNR of the spectra. The experimental factors chosen for the collection of all spectra, with and without TCF material are shown in Table 3.4.

Table 3.4 Factors used in TCF spectral analysis

Experimental Factors	**Details**
Tube Voltage (kVp)	60, 70, 80, 90 and 100
Tube Current . Exposure Time (mAs)	400, repeated 4 times total of 1600 mAs
Focal Distance (cm)	20
Lucite Rod Diameter (mm)	4
Number of MCA channels	256

The selected factors were a compromise between low SNR and resolution. The 4 mm diameter Lucite rod and MCA 256 channels, selected for this study, increased SNR and decreased resolution. Resolution is determined by the energy window width or the range of energies that could be recorded in a single MCA channel. The energy window width, using the maximum number of MCA channels, was 0.0537 keV with the selected energy range of 0.1 to 110 keV. Using 256 MCA channels, the energy window width was increased by a factor of eight to approximately 0.429 keV. Resolution was decreased by a factor of eight from the maximum possible resolution of the MCA. Overall noise was increased with the use of the 4 mm diameter Lucite rod.

Exposures were made with and without the presence of TCF material. A total of 150 spectra were collected and recorded. The Compton spectra were deconvolved to represent the original beam spectrum.

Background radiation was recorded in each x-ray room where the units were located. The collection time for the background radiation was 5 minutes. Five minutes was the typical time taken to record each spectrum. This allowed time for x-ray tube cooling between the four exposures required for each spectrum's data collection. Background radiation data were then subtracted from each regenerated spectrum.

Methods to reduce visible noise within the spectra for display purposes were evaluated. After evaluating several signal filtering techniques, the filter selected was the Savitzky-Golay filter as modified by Gander & von Matt (1995). Russ (1995) also recommends this technique for the smoothing of one-dimensional signal profiles

of x-ray spectra. The modified Savitzky-Golay filter algorithm allows user input to modify matrix size and vector length within the algorithm. Matrix size and vector length were chosen to optimise spectral appearance for noise reduction while maintaining resolution. A comparison of x-ray beam spectra with and without the Savitzky-Golay filter is shown in Figure 3.9. Other filters evaluated, such as an averaging filter, used the mean value of a range of spectrum values. Where spectrum values represent a peak such as the K_α and K_β characteristic radiation peaks, at approximately 59 keV and 67 keV respectively, in Figure 3.9, the averaging filter smooths the peaks. The Savitzky-Golay preserves the peaks yet smooths the noise variations.

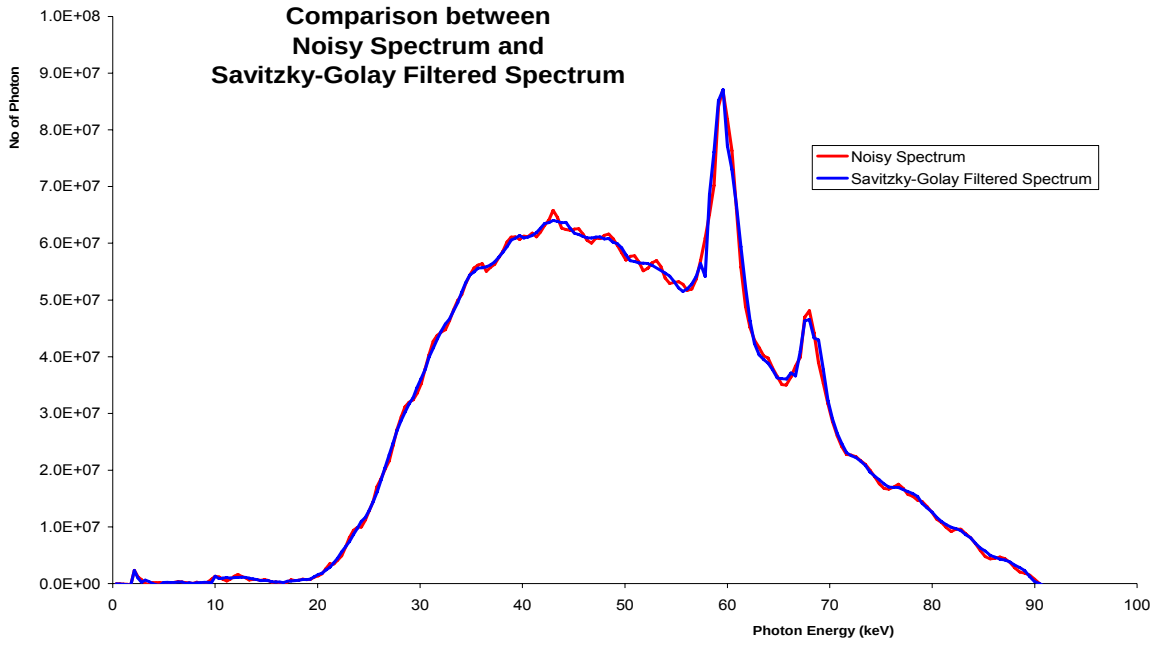

Figure 3.9 Effect of Savitzky-Golay filter on a noisy spectrum

The spectral data modified by the modified Savitzky-Golay filter algorithm were for display purposes only. All spectral plots displayed in this chapter were modified using the modified Savitzky-Golay filter algorithm. Later analysis of the spectral data was undertaken prior to the modification of the data with the modified Savitzky-Golay filter algorithm.

Visual comparison of the unfiltered x-ray spectra from the three x-ray units is provided in Figure 3.10. Unit 1 has a higher photon output number at each photon

energy than the other two units for the same radiographic exposure factors of 100 kVp, 4 x 400 mAs and 20 cm distance. X-ray Unit 3 (100% ripple) would require an increase in mAs to achieve the same optical densities on the film as Unit 1 (1% ripple). The spectral profiles also differ between the three units. These differences are due to the difference in generator ripple and total filtration between each unit. Unit 3 also shows maximum photon energy of approximately 97 keV although the kVp set on the unit was 100. This unit required recalibration to adjust the kVp setting to the output energies emitted.

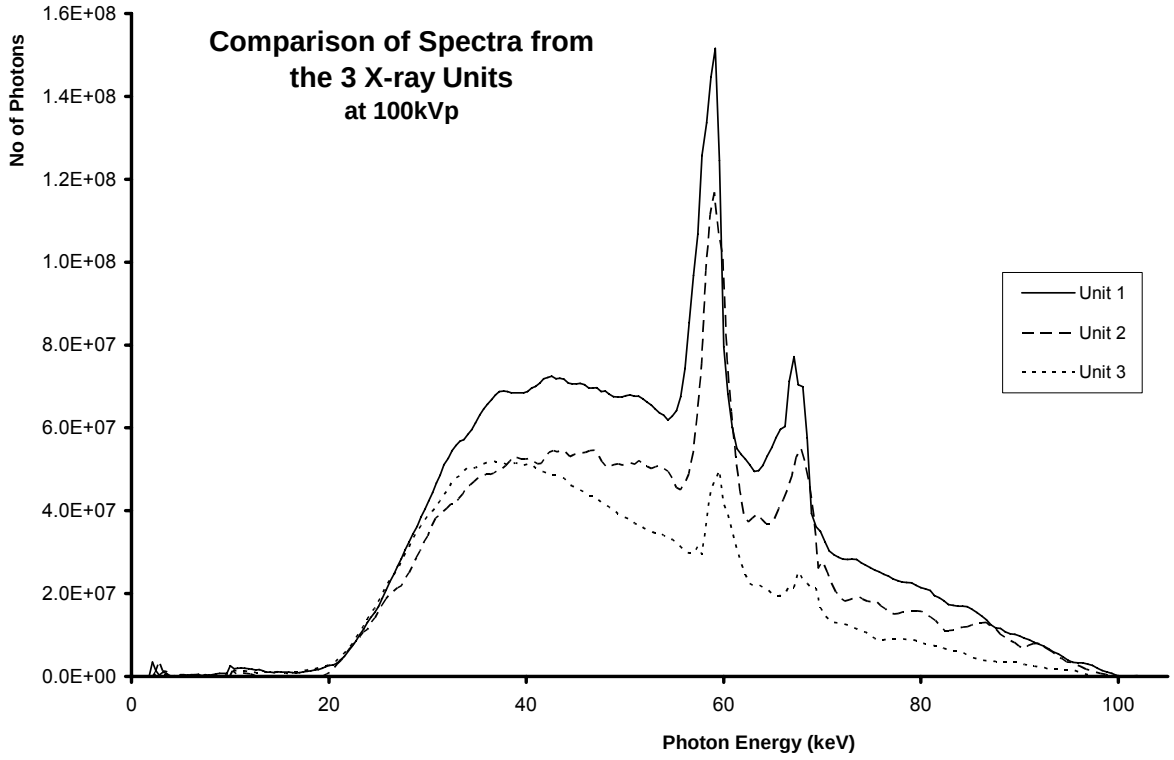

Figure 3.10 Comparison of unfiltered spectra from the 3 x-ray units

Examples of the x-ray spectra with and without the addition of TCF material into the x-ray beam are shown in Figure 3.11a, b & c. Figure 3.11a. shows spectra with lead acrylic TCF filter material added in the x-ray beam. Figures 3.11b. & c. have added TCF material of aluminium composite and silicone rubber respectively.

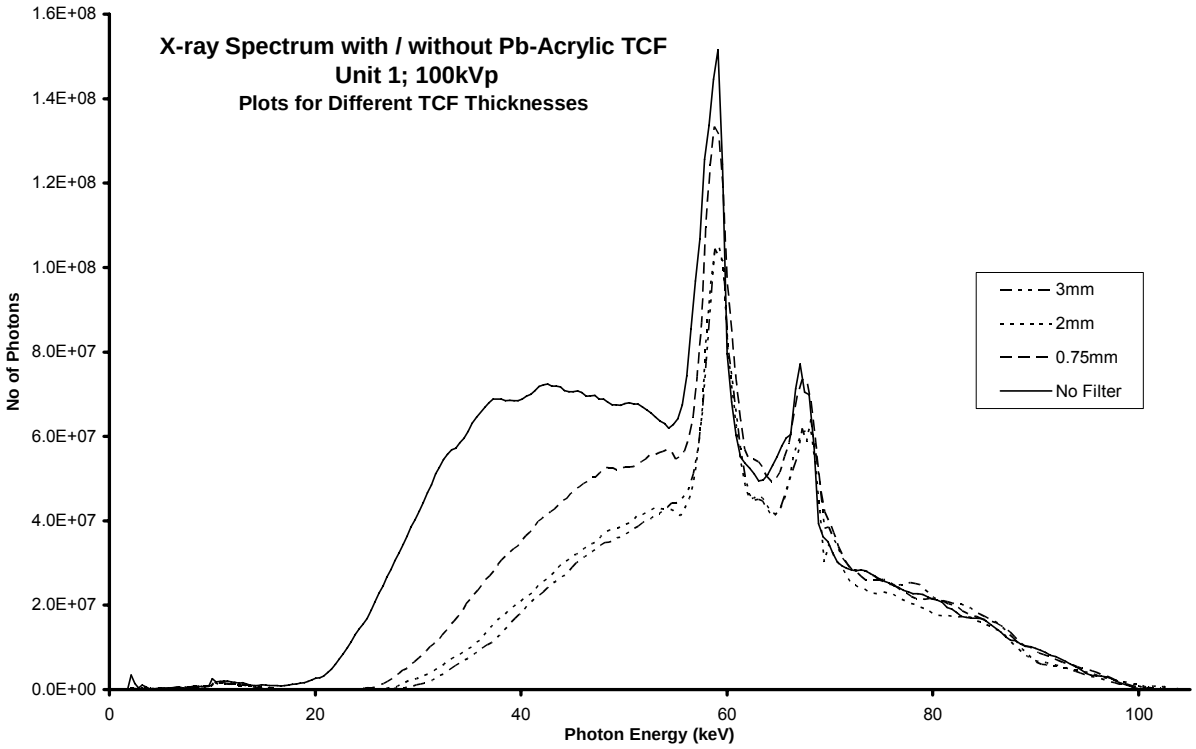
X-ray Spectrum with / without Pb-Acrylic TCF
Unit 1; 100kVp
Plots for Different TCF Thicknesses
No of Photons
Photon Energy (keV)
3mm
2mm
0.75mm
No Filter
1.6E+08
1.4E+08
1.2E+08
1.0E+08
8.0E+07
6.0E+07
4.0E+07
2.0E+07
0.0E+00
0
20
40
60
80
100

a.

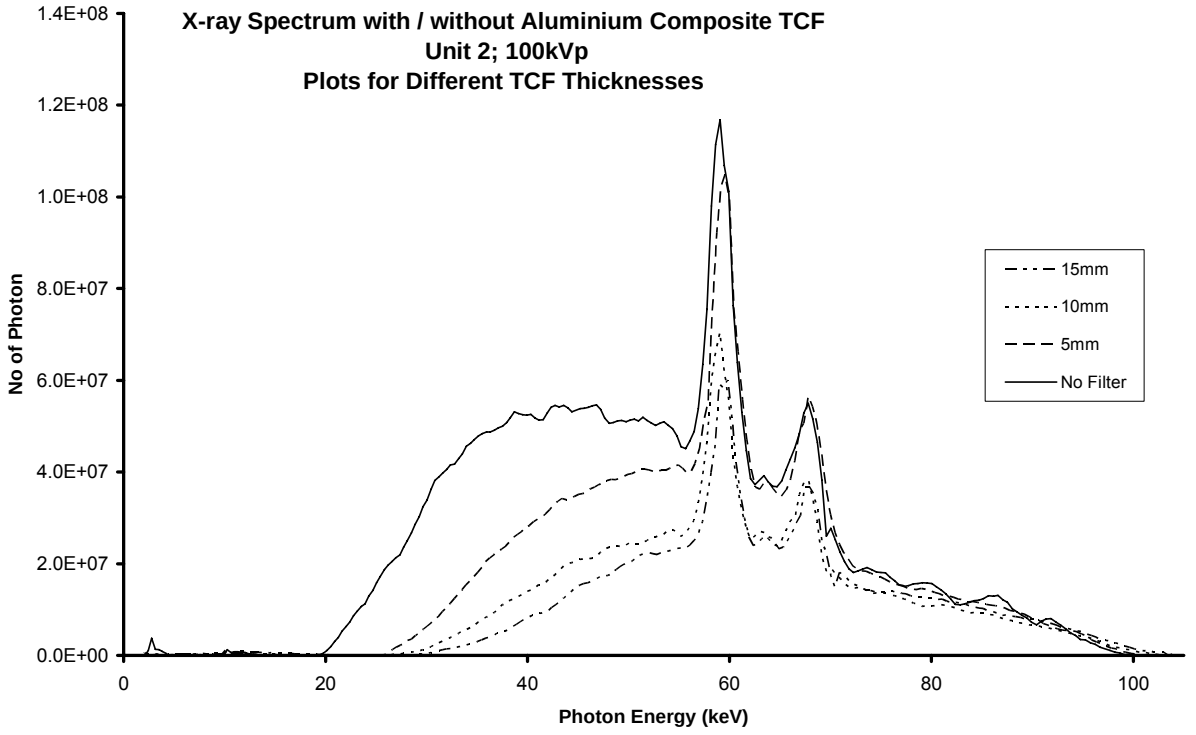
X-ray Spectrum with / without Aluminium Composite TCF
Unit 2; 100kVp
Plots for Different TCF Thicknesses
No of Photon
Photon Energy (keV)
15mm
10mm
5mm
No Filter
1.4E+08
1.2E+08
1.0E+08
8.0E+07
6.0E+07
4.0E+07
2.0E+07
0.0E+00
0
20
40
60
80
100

b.

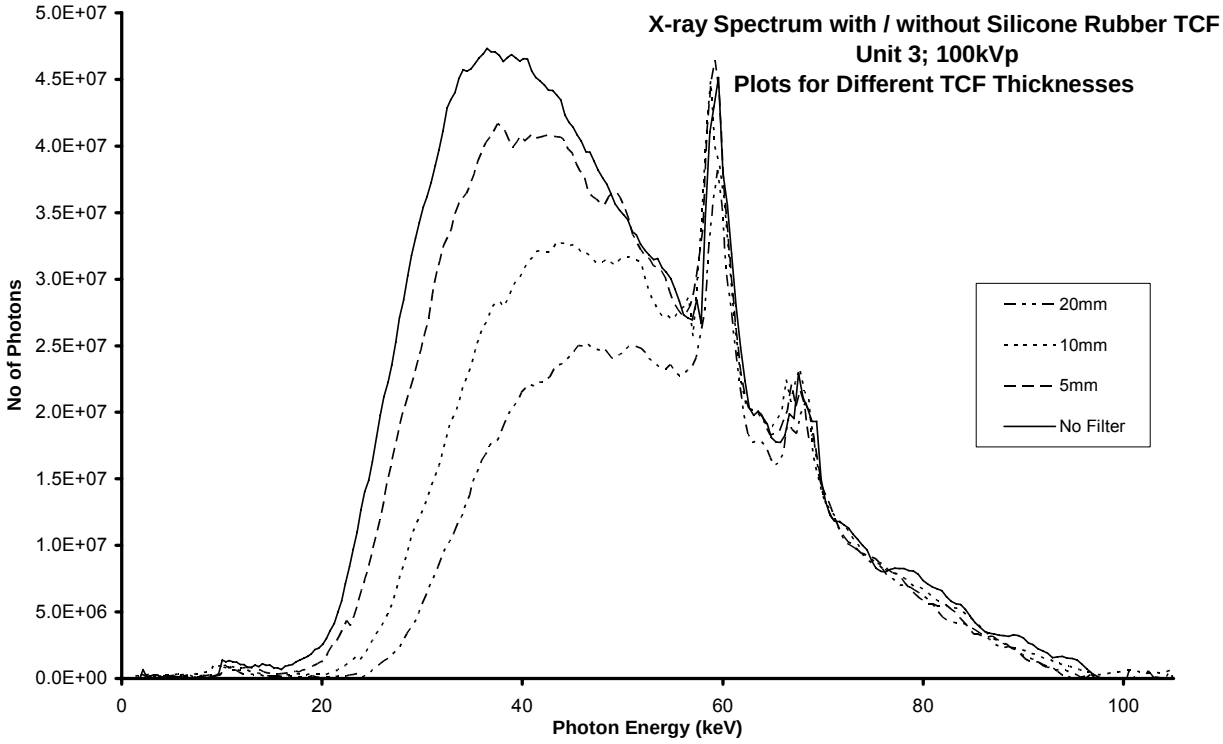

c.

Figure 3.11 Examples of unfiltered and various TCF thickness spectra from the 3 x-ray units:

a. Lead acrylic TCF material
b. Aluminium composite TCF material
c. Silicone rubber TCF material

Figures 3.11a, b & c show that increasing the thickness of all three TCF materials resulted in increased attenuation of the x-ray beam. Evaluation of the effect of TCF material type on x-ray beam attenuation using the spectral plots is subjective. Objective measurements of linear attenuation coefficients and HVL were made.

3.7 Linear Attenuation Coefficients of TCF Materials

Linear attenuation coefficients of the three TCF materials at various photon energies were calculated. Linear attenuation coefficients are a measure of the likelihood of attenuation for a given material at given photon energy. The relationship between linear attenuation coefficient, entrance and exit beam intensities and material thickness is given in Equation 3.2.

$$I = I_o.e^{-\mu.x} \qquad \text{…….. 3.2}$$

where: I is the exit photon intensity from the material;

I_0 is the entrance photon intensity;

x is the thickness of the attenuating material;

μ is linear attenuation coefficient of the material at a given photon energy.

The change in intensity of the beam as it transits the material is an exponential decay. The linear attenuation coefficient is dependent upon the effective atomic number of the material, material density, ρ, and the photon energy. Mass attenuation coefficient is often used as a measure of attenuation as it is independent of material density. It is calculated as μ/ρ. Where the material density cannot be readily determined, the linear attenuation coefficient is a more useful measure of attenuation of a given material (Bushong, 2001; Curry *et al*, 1990; Dowsett *et al*, 1998; Thompson *et al*, 1994).

Linear attenuation coefficients were calculated at three photon energies, 35 keV, 50 keV and 65 keV. These selected energies provide a range of energies typically found in a clinical x-ray beam. Photon counts at these energies were recorded from the previously discussed spectral data. For the purpose of calculating μ using Equation 3.2, I_0 was the photon count obtained from spectra without the TCF material present and I was the photon count obtained using the various thicknesses of TCF material. The values of I_0 and I were averaged across the three x-ray units and also across three selected kVp settings of 80, 90 and 100 kVp.

Graham (2001) provided an improved method for the calculation of the exponential regression coefficients, so as to determine μ in Equation 3.2. A common method of fitting an exponential function, $y = a.e^{bx}$, to data is to calculate the natural logarithms of the y data so now $\ln y = \ln a + b.x$. Linear regression is then performed on the log values to determine the slope of the regression line, b. Graham's (2001) preferred method is to predict a value of y with a "guess" value of b. The square of the errors between the actual y values and the predicted y values are calculated. Using Microsoft® Excel solver function, the "guess" is altered until the sum of the square of the errors is minimised. Graham showed that this was a more accurate method of fitting an exponential curve to the measured values. This method was used to calculate μ.

Table 3.5 lists the μ, measured in cm^{-1}, at photon energies of 35, 50 and 65 keV for lead (Pb) acrylic, aluminium composite and silicon rubber TCF material. Figures 3.12a, b & c provide a graphic representation of the relative intensities (I/I_0) at each TCF material thickness and the exponential regression curves of best fit for the measured data. Error bars are shown as +/- 1 standard deviation. Coefficients of determination (R^2) are provided in Table 3.1 and in the figures. The coefficient of determination is the square of the correlation coefficient R and it provides a measurement of how well the exponential model explains the variance in the measured data. An R^2 value of 1.0 indicates that the data perfectly follow an exponential curve (Keller, 2001).

Table 3.5 Linear attenuation coefficients (μ in cm^{-1}) for each TCF material with corresponding coefficients of determination

Photon Energy (keV)	35		50		65	
TCF Material	μ (cm^{-1})	R^2	μ (cm^{-1})	R^2	μ (cm^{-1})	R^2
Silicone Rubber	0.6849	0.894	0.2097	0.896	0.1319	0.963
Aluminium Composite	1.8600	0.994	0.6341	0.893	0.2687	0.857
Lead Acrylic	8.2931	0.962	2.3384	0.920	0.7059	0.947

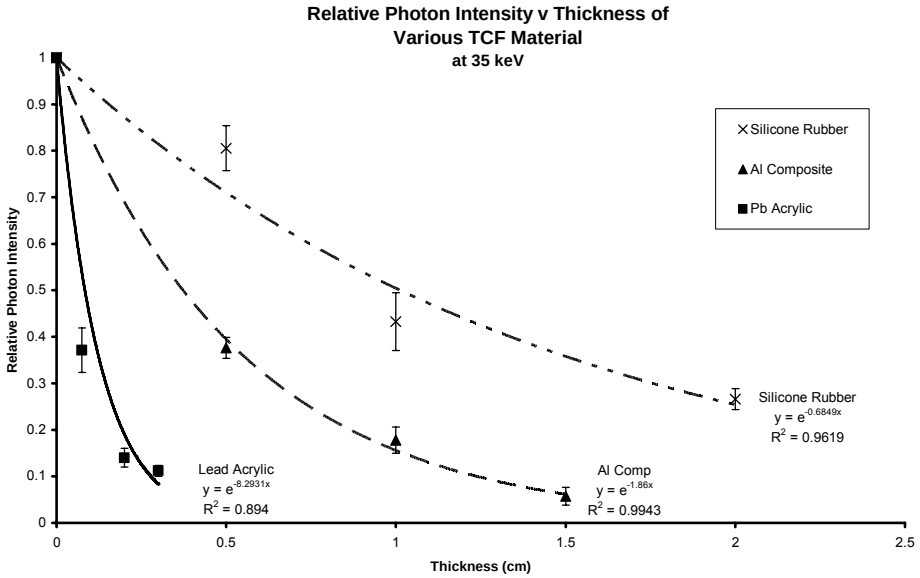

a.

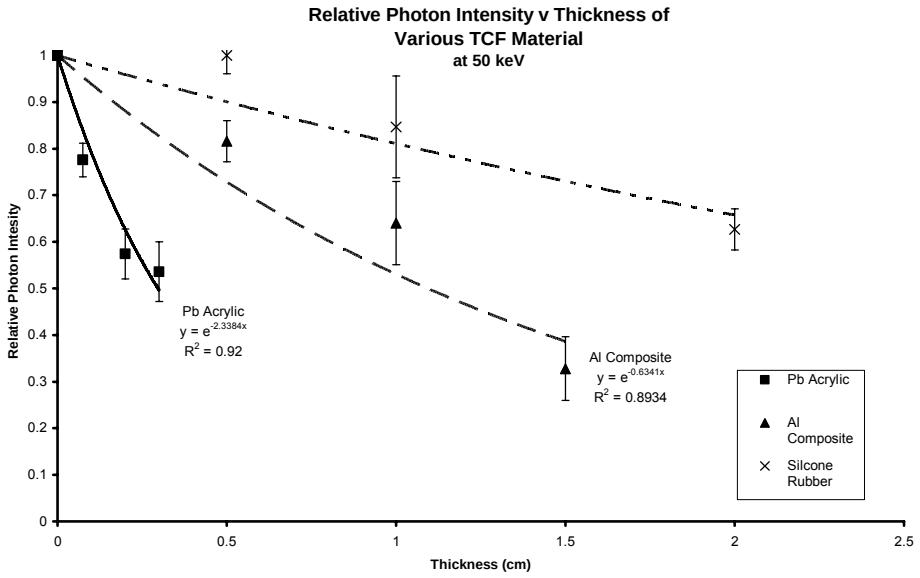

b.

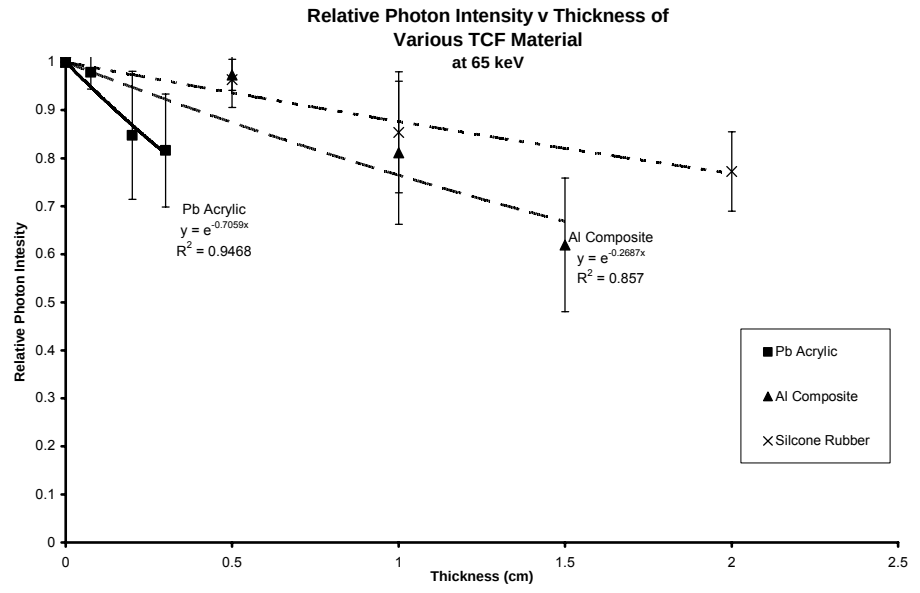

c.

Figure 3.12 Relative intensity plots for Pb acrylic, Al composite and Silicon rubber TCF material thicknesses at a. 35 keV; b. 50 keV; c. 65keV

The calculated μ of the three TCF materials were compared with the known μ of various materials. Linear attenuation coefficients of selected materials were converted from the mass attenuation coefficient and density data provided by Hubbell & Seltzer (1996). Table 3.6 provides μ of selected materials at 30, 50 & 60 keV.

Table 3.6 Linear attenuation coefficients (μ in cm^{-1}) at 30, 50 & 60 keV for various materials (adapted from Hubbell & Seltzer, 1996)

	μ (cm^{-1})		
MATERIAL	30 keV	50 keV	60 keV
Copper	97.8432	23.41248	14.27328
Glass, Borosilicate (Pyrex)	51.4015	13.67882	8.56989
Calcium	6.32400	1.57945	1.01959
Aluminium	3.04447	0.99350	0.74978
Bone, Cortical	2.55552	0.81446	0.60442
Bone-Equivalent Plastic	1.41404	0.50837	0.39701
Carbon, Graphite	0.43554	0.31807	0.29801
A-150 Tissue-Equivalent Plastic	0.39231	0.24772	0.22630
Muscle, Skeletal	0.39722	0.23751	0.21504
Water, Liquid	0.37560	0.22690	0.20590
Adipose Tissue	0.29099	0.20169	0.18753

For comparison to the materials listed in Table 3.6, lead acrylic TCF material has a greater ability to attenuate x-ray photons than pure calcium but less than borosilicate glass (Pyrex). The aluminium composite TCF material has a μ greater than that of carbon but less than that of pure aluminium. Silicone rubber TCF material has similar attenuation characteristics to skeletal muscle and to A-150 tissue equivalent plastic material used to mimic human muscle in dosimetry research.

3.8 Half Value Thicknesses of TCF Material

The half value thicknesses of the three TCF materials were calculated for the three x-ray units. Linear attenuation coefficients are a measure of the material's attenuating ability at specific photon energies. X-ray beams are polyenergetic. The HVT of a material provides a more useful measure of the material's attenuating ability in a polyenergetic x-ray beam. HVT varies between x-ray units, depending on the x-ray unit's generator ripple and its inherent and added filtration (Bushberg *et al*, 2002; Curry *et al*, 1990; Dowsett *et al*, 1998).

The method typically used to determine the HVT in polyenergetic x-ray beams is to place various thicknesses of attenuating material in the x-ray beam and determine the thickness that reduces the exit intensity of the beam to half of the entrance intensity. Various thicknesses of TCF materials were placed in the beam for spectral measurement. These spectra were used for determination of the HVT for each of the x-ray units.

The HVT of a monoenergetic x-ray beam can be calculated by modifying Equation 3.2. The formula in Equation 3.3 (Dowsett *et al*, 1998, p. 110) is used to determine the HVT of a monoenergetic x-ray beam. It can also be used to determine the HVT of a polyenergetic x-ray beam. The factor μ for polyenergetic x-ray beams is not a true value of linear attenuation; rather it is an "averaged" value of attenuation for that particular x-ray beam.

$$\frac{I}{I_o} = 0.5 = e^{-\mu.HVT} \quad \text{..... 3.3}$$

where: I is the exit photon intensity from the material;

I_0 is the entrance photon intensity;

HVT is the thickness of attenuating material that attenuates the beam to half of I_0;

μ is the "averaged" linear attenuation coefficient of the polyenergetic x-ray beam.

The number of photons in the x-ray beam is a measure of its intensity (Bushberg *et al*, 2001). The area under the spectrum curve represents the total number of photons. The sum of the photon counts for each spectrum hence provides a measure of the beam's intensity. Intensity measurements were recorded for each TCF material thickness at each kVp setting. The ratios of intensities with and without TCF material were calculated.

Calculations of μ, using Equation 3.2, for the TCF materials in polyenergetic x-ray beam were made using the method described by Graham (2001). Following the calculations of μ, values of the HVT for each TCF material, kVp setting and x-ray unit were determined using Equation 3.3. The calculated HVT values can be seen in Table 3.6. Plots of attenuation curves at 100 kVp for each TCF material are shown in Figures 3.13a, b & c. The horizontal lines in these figures represent half of I_0 and the vertical lines provide a graphical representation of the HVT for each x-ray unit. A graphical comparison of the HVTs for TCF materials at 90 kVp in the three x-ray units is provided in Figure 3.14. In this figure the horizontal line also represents half of I_0 and the vertical lines provide a graphical representation of the HVT for each TCF material.

Table 3.6 Half value thicknesses (cm) of TCF material for x-ray units 1, 2 and 3

kVp	100	90	80	70	60
HVT of Silcone Rubber (cm)					
Unit 1	2.25	2.07	1.56	1.25	0.96
Unit 2	1.60	1.27	1.24	1.05	0.69
Unit 3	1.86	1.70	1.33	1.21	0.90
HVT of Al Composite (cm)					
Unit 1	1.02	0.91	0.74	0.67	0.54
Unit 2	0.81	0.75	0.66	0.45	0.43
Unit 3	0.94	0.78	0.70	0.54	0.41
HVT of Pb Acrylic (cm)					
Unit 1	0.243	0.173	0.150	0.141	0.092
Unit 2	0.162	0.151	0.121	0.088	0.086
Unit 3	0.175	0.171	0.149	0.104	0.066

X-ray Units 2 and 3 had similar HVT values, especially for the lower kVp settings of 60 and 70 kVp. The HVT value in x-ray unit 1 for all TCF materials was always larger than in the other two units. The generator ripple varied greatly between x-ray units 2 and 3, approximately 3.5% and 100% respectively. The additional added filtration in unit 3 (see Table 3.5) increased the effective energy of the beam to produce similar HVTs for the TCF materials in units 2 and 3.

The calculated HVT values provided better knowledge of the characteristics of the different TCF material. This knowledge could be used to improve selection of an appropriate filter material and the thickness of that material needed to compensate for a patient's anatomy.

The measured values of HVT are unique to the x-ray units used in this study. Knowledge of an x-ray unit's generator ripple and amount of added filtration provides some general information about the performance of different TCF materials in typical clinical situations.

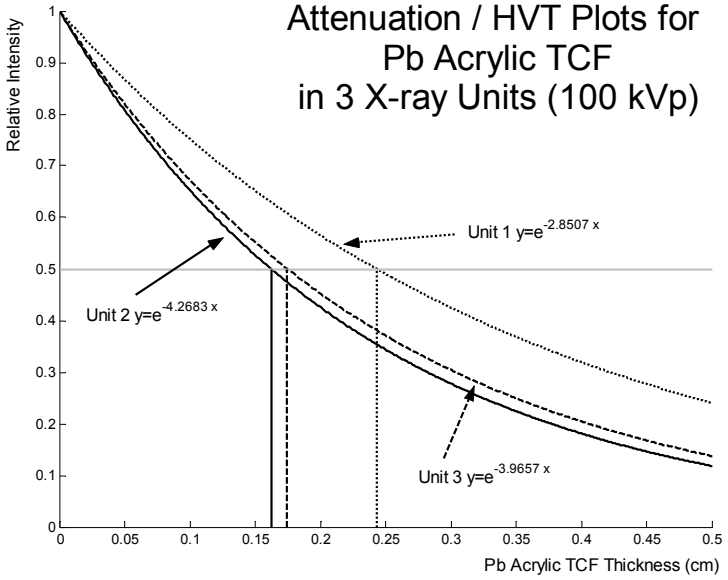

a.

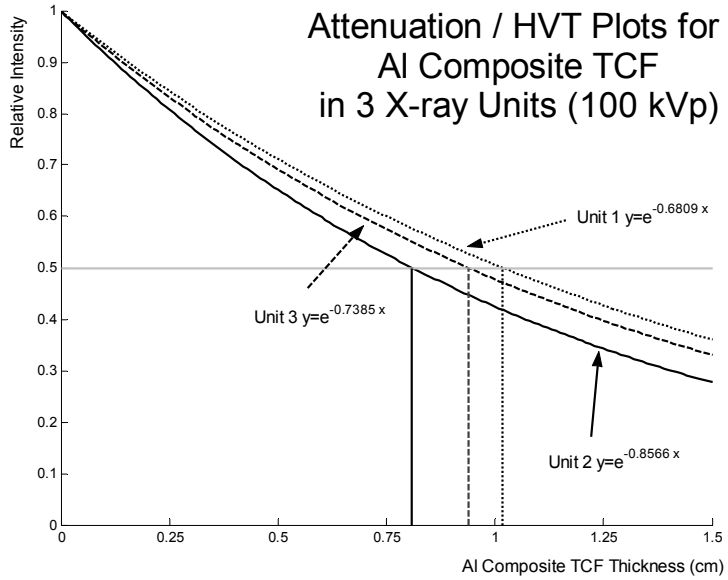

b.

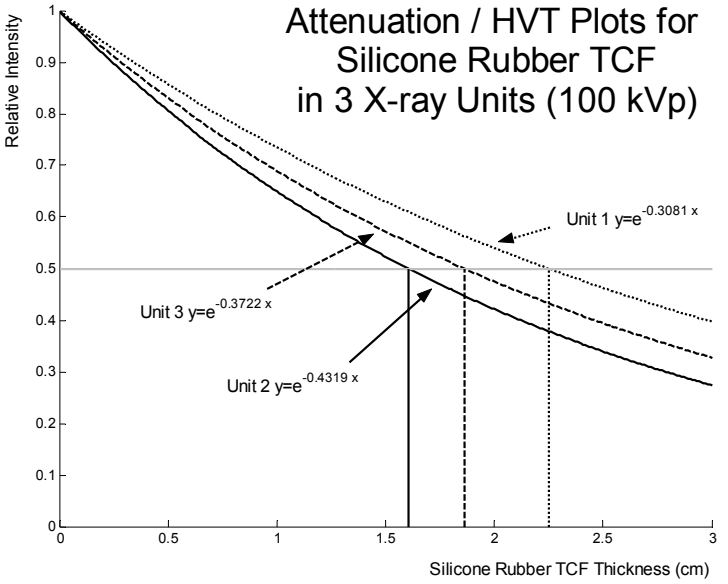

c.

Figure 3.13 Attenuation / HVT plots for TCF material in units 1, 2 & 3 at 100 kVp:
a. Pb acrylic; b. Al composite; c. Silicon rubber

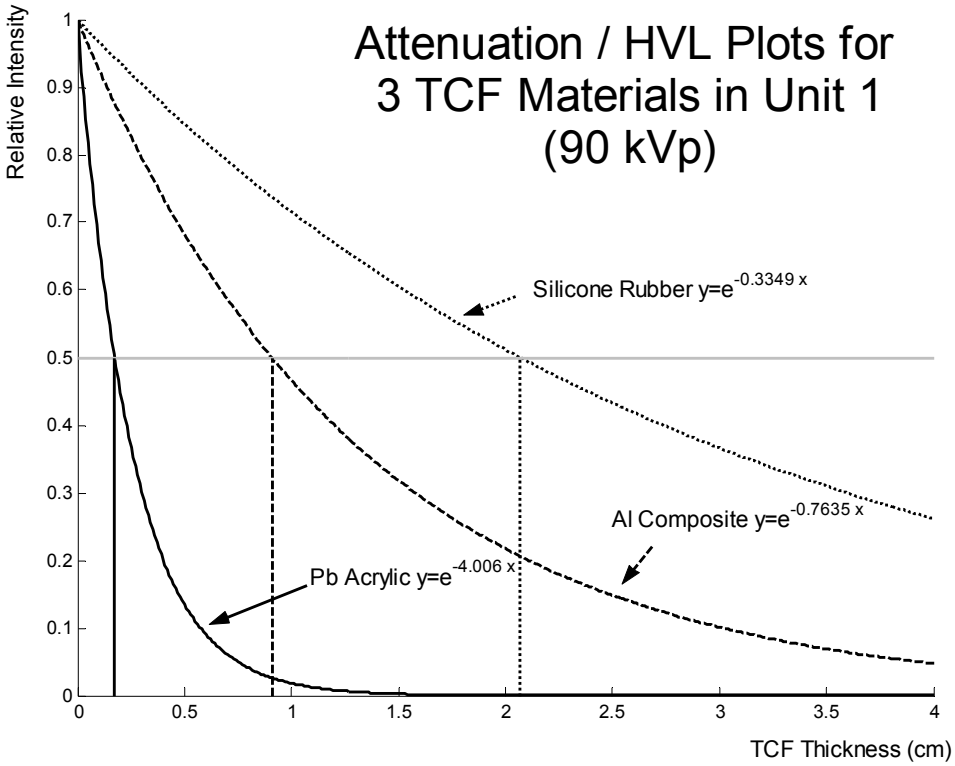

Figure 3.14 Attenuation / HVT plots for Pb acrylic, Al composite & Silicon rubber TCF material in unit 1 at 90 kVp

Alternative methods of data analysis of the spectra were undertaken and have been reported elsewhere (Davidson, 2001). In that paper, conclusions were drawn as to the most appropriate kVp settings and type of x-ray unit for the use of each of the TCF materials. The approaches undertaken here represented a clinical focus. This paper can be found in Appendix 1.

The knowledge gained from measuring the spectral data and calculating the linear attenuation coefficients and HVL of the TCFs provided the basis for development of anatomically shaped RCMs. This development and the use of the RCMs in digital radiography is discussed in Chapters 6 and 7.